Desalination and Water Treatment
www.deswater.com
doi: 10.5004/dwt.2021.27211

225 (2021) 231–243
June

Potential recycle of industrial waste towards economic adsorbent preparation for effective removal of toxic elements

Raed E-S Rihan[a], Mohamed M. Abo-Aly[a], Mohamed F. Attallah[b,*]

[a]*Chemistry Department, Faculty of Science, Ain Shams University, Egypt, Tel. +01067026041; email: raedrihan@yahoo.com (R.E-S. Rihan), Tel. +20 1141534022; email: aboalymo@yahoo.com (M.M. Abo-Aly)*
[b]*Analytical Chemistry and Control Department, Atomic Energy Authority of Egypt, 13759 Cairo, Egypt, Tel. +20 1007730930; email: dr.m.f.attallah@gmail.com*

Received 30 September 2020; Accepted 4 March 2021

ABSTRACT

Activated carbon prepared from sawdust, an inexpensive biowaste of the wood industry, to remove Pb^{2+}, Co^{2+}, and Cd^{2+} ions from water solutions was examined in batch experiments. Batch studies were conducted to study the impact of some factors like pH, contact time, the metal ions concentration, and temperature on adsorption efficiency. The results indicated that the optimum conditions for Pb^{2+}, Co^{2+}, and Cd^{2+} ions removal at pH 6 and an equilibrium contact time of 90 min. Adsorption isotherms such as Freundlich and Langmuir were estimated. It is turned out that the sorption obeys the Langmuir model, and the extreme sorption capacity of Pb^{2+}, Co^{2+}, and Cd^{2+} was 50.65, 15.53, and 12.54 mg/g, respectively. Thermodynamic factors like $\Delta H°$, $\Delta S°$, and $\Delta G°$, for sorption Pb^{2+}, Co^{2+}, and Cd^{2+} have been calculated. The thermodynamic data demonstrated that the sorption of metal ions endothermic and spontaneous. Desorption studies show that the used adsorbent may be regenerated in HCl and HNO_3. The efficacy of the sorbent in the treatment of surface and groundwater metal ions and some organic pollutants has been investigated. The results revealed that the used adsorbent has been successful a promising material for treating some contaminants.

Keywords: Sorption; Activated carbon; Biomass sawdust; Water treatment; Heavy metals

1. Introduction

Water is the most critical compound on the earth for life, and it is a tremendous global challenge for the 21st century to possess drinkable water. Pure and unpolluted water is a fundamental requirement for all living organisms [1]. Water pollution with heavy metals is the most critical ecological troubles because of their poisonous nature [2], not biodegradable and tend to concentrate on living things, resulting in various disorders and unrest like headache, dizziness, nausea, vomiting, chest pain, dry cough, chest tightness, rapid breathing, shortness in respiration, nephritis, acute weakness, central nervous system damage, cancer, lung damage, the brain damage and eventually results in death [3]. Therefore, it is vital to eliminate the heavy metal ions before they are discharged into the environment [4].

Heavy metals are produced from different industries, and the most essential are: mining and smelting, electrolysis, nuclear energy industries, metallurgical, tannery, cosmetics, insecticides, photography, textiles, paints, dyes, and battery industries. Heavy metals are categorized into three different types: poisonous metals, valuable metals, and radioactive metals [5]. According to the World Health Organization (WHO), some metals, such as aluminum, chromium, cobalt, cadmium, zinc, nickel, copper, lead, and mercury, are considered poisonous metals [6].

* Corresponding author.

The most extensively used strategies for metal ions removal from wastewater involve chemical precipitation/co-precipitation, advanced oxidation processes, exchange of ion, electrochemical treatment, technologies of the membrane, photo-catalysis, reduction, adsorption, flocculation, membrane filtration, reverse osmosis, and so on., had been suggested inside the literature [7]. Among these technologies, adsorption is a preferable strategy for metal removal from wastewater because of its simplicity in performance, non-toxic, high efficacy, competitively priced, low investment, fast, eco-friendly, and universal [7–9].

One of the most effective and dependable physicochemical methods is the adsorption with activated carbon [10]. Even so, activated carbon commercially available is typically produced from coal or wood and is thus reasonably costly [11]. Therefore, it is essential to make low-priced and productive carbon used to control water contamination. Extensive diversity of very cheap materials and agricultural waste products is used to eliminate heavy metals from aqueous solutions, involving peat [12], palygorskite [13], modified soda lignin [14], saffron leaves [15], waste olive stones [16], walnut shell [17], coconut husk [18], tobacco stem [19], coffee husk [20], pistachio shell carbon [21]. In Egypt, there are large amounts of agricultural wastes that pose a solid contaminant to the ecosystem.

The sorbent sawdust is one of the most promising. It was commonly utilized for heavy metals removal and some other undesirable substances from aqueous solutions [22]. Since it is available in redundancy, renewable, sustainable sources, large production, and very cheap [23,24], wealthy in cellulose, lignin, and hemicellulose to be utilized for adsorbing heavy metal ions from wastewater [25]. If such materials are treated with thermal and/or chemical methods, the efficiency of removing heavy metals with the raw cellulosic biomass may be increased considerably [26]. Therefore, sawdust is one of the most critical agricultural biomasses that may serve as prospect sorbents to remove various contaminants, particularly metal ions.

There are fundamentally two procedures for activated carbons preparation: chemical activation and physical activation [27]. Chemical activation produces extremely adsorbents by groups of activating agents like: NaOH, KOH, K_2CO_3, H_3PO_4, $ZnCl_2$ [28] because it produces biocarbon, which is characterized by highly developed surface area, and pore size distribution required [29]. Amongst the chemical activating agents, phosphoric acid (H_3PO_4) is eco-friendly because it is non-contaminant, is readily washed off with water, and may be recycled back into the process [30]. Physical or gas activation includes increasing porosity by gasifying at comparatively high temperatures with an oxidizing agent; the widespread activation agents are carbon dioxide, steam, or their combination [31]. The most popular activating agents are CO_2, and steam since the reaction's endothermic behavior makes the process easier to control. In general, the utilization of CO_2 is favored because the reactivity of CO_2 becomes low at extreme temperatures making the activation process easy to control [27].

The world production concerning quicklime (calcium oxide) is evaluated at about 350 million tons. The steel industry globally utilizes somewhere in the range of 140 to 160 million tons of quicklime. A large part of quicklime production is manufactured in captivity in steel factories, where it is necessary raw material for steelmaking [32]. Furthermore, quicklime is a crucial component of technology used in a wide range of industries, including agriculture activities, construction, disinfection, food processing, plastics, SO_2 post-combustion capture, water treatment, and sugar refining [33], leather tanning processes [34], fungicides [35] and soil stabilization by adding burned limestone products either calcium hydroxide or quicklime [36]. Moreover, calcium oxide is that the principal ingredient in traditional Portland cement [37]. Calcination of limestone at 800°C produces quicklime [38]. During the calcination process, a massive quantity of CO_2 is emitted [39]. If the CO_2 released during the calcination process is expelled directly into the air, it leads to the "greenhouse effect" with reciprocal impacts on the natural ecological systems and humanity. As a result, the effective re-use of the expelled CO_2 generated during the calcination process is one of the main strategies for avoiding its emission through the atmospheric air. The activation of activated carbon using the CO_2 effluent can fulfill the criteria of a sustainable green, relatively clean process [40].

The purpose of this work was aimed to explore the possibility of Pb^{2+}, Co^{2+}, and Cd^{2+} ions removal from aqueous media via sawdust modified with phosphoric acid and carbon dioxide produced from the calcination of limestone. The optimum conditions were examined to achieve maximum adsorption using such materials. The consumption of a part of biomass in this application protects the environment from another form of contamination resulting from biomass's discarding. Batch experiments are carried out for kinetic studies on the decontamination of Pb^{2+}, Co^{2+}, and Cd^{2+} from aqueous media. The effect of different parameters like change in pH during sorption, temperature, initial concentration, and contact time was examined. Pseudo-first-order, second-order, Freundlich and Langmuir equations are used to assess the adsorption mechanisms. The relevant thermodynamic factors, namely: $\Delta G°$, $\Delta S°$, and $\Delta H°$, have been determined and defined.

2. Materials and methods

2.1. Materials

The used reagents in all experiments were of analytical grade (AR) and used without further purification. Cobalt nitrate, lead nitrate, and cadmium nitrate were purchased from Merck (Darmstadt, Germany). Calcium carbonate, sodium hydroxide, phosphoric acid, and hydrochloric acid were procured from PanReac. Sawdust was obtained from the workshop of the local timber industry. De-ionized water was used to prepare the solutions during experimental work.

2.2. Adsorbent preparation

The sawdust was obtained from the workshop of the local timber industry in Sharkia Government, Egypt, and rinsed with de-ionized water to remove impurities. The sawdust was washed to avoid leaching of color as well as other impurities till a clear solution was produced. Eventually, overnight, the cleaned sample was dried at 100°C ± 5°C. To activate the surface sites of sawdust phosphoric acid (H_3PO_4), 70% was used. In this experiment, 150 g of sawdust was soaked in 100 mL 70% phosphoric acid. The sample was agitated slightly to guarantee acid penetration within. Then, the mixture's temperature was fixed at 80°C for overnight to assist in the precursor's proper wetting and impregnation. Then adding 50 mL (10%) Calcium carbonate to the impregnated mass, then inserted into the ignition tube, which was then put open from both ends in a tubular electric furnace. The temperature had been raised to the necessary end temperature at a rate of (50°C/10 min). The carbonization process was conducted for 1 h at a temperature of 800°C. Hot de-ionized water washed over the sample. The washing process was repeated four times and immersed overnight in 1 percent $NaHCO_3$ solution to eliminate the remaining acid, followed by drying overnight at 110°C. Eventually, the sample was cooled at room temperature and ground to develop powdered sawdust activated carbon (SAC).

2.3. Adsorption studies

The batch equilibrium method was used to conduct adsorption experiments. Tests were conducted by stirring 0.25 g of sorbent using an orbital shaker with 50 mL (50 mg/L) of adsorbing solutions. Samples were shaken at time periods and filtered with filter paper (Whatman). The filtrate solution was analyzed with atomic absorption for the residual concentrations Pb^{2+}, Co^{2+}, and Cd^{2+}. Adsorption isotherm and kinetic experiments with specific initial concentrations of Pb^{2+}, Co^{2+}, and Cd^{2+} ions were performed by maintaining the sorbent dose at a constant level. All experiments were done in triplicate to avoid any inconsistency in experimental results, and the calculated uncertainty does not exceed 5%. In the aqueous phase before and after the experiment, sorption capacities were determined from the difference in the metal ion concentrations according to Eq. (1) while the uptake % was calculated according to Eq. (2):

$$q_e = \left(C_0 - C_e\right)\left[\frac{V}{m}\right] \tag{1}$$

where q_e sorption capacity per unit mass of sorbent (mg/g); C_0 initial metal ions concentration (mg/L); C_e the final concentration of metal ions at equilibrium (mg/L); M sorbent mass (g); V sample volume (L).

$$\%\text{Removal} = \frac{\left(C_0 - C_e\right)}{C_0} \times 100 \tag{2}$$

2.4. Characterization of sorbent

The characterization of SAC was performed by scanning electron microscope (SEM) Model JSM-5600 LV, JEOL, Japan, attached to an Oxford Inca EDX detector, and the FTIR spectrometer (8000s, Thermo-Scientific, USA) with a range from 400 to 4,000 cm^{-1} by the potassium bromide disc technique. The pH values of various solutions were calculated by digital pH meter, Thermo-Scientific USA instruments. Atomic absorption (AA), Varian AA240FS, Austria, gas chromatography (GC) Varian, CP-3800, Column CPSIL 19, USA, and Cecil 7400 Double Beam UV/Vis spectrophotometer were used to measure metal ions concentrations and organic contaminants. Shaking of samples was performed using an orbital shaker, Thermo-Scientific, UK.

3. Results and discussion

3.1. Characterization of sawdust activated carbon

Fourier-transform infrared (FTIR) spectra of SAC before and after adsorption are presented in Fig. 1, denoting many extreme peaks on the sorbent surface, specific to various important functional groups. It is noted that the peak at 3,427 cm^{-1} is due to the O–H stretching vibration [41]. The peaks appear at 2,922.17 and 2,854.71 cm^{-1} were linked to the C–H stretching in methyl and methylene groups [42], while the band appears at 1,646 cm^{-1} refers to the existence of C=C bond [43]. The appearance of the peak around 1,569.93 cm^{-1} allotted to the C=O stretching vibration may attribute to lignin and hemicelluloses [42]. The band at 1,413.72 cm^{-1} may be due to COO– groups [44]. The peak that appears at 1,384.37 cm^{-1} may attribute to the oxygen functional groups as C=O carboxylic stretching group [45]. The band at 1,039.89 cm^{-1} was assigned to C–O of the cellulose [46]. The band seen at 702.48 cm^{-1} may attribute to functional group C–O–C of esters, phenol, or ether [47], while the band seen at 469.21 cm^{-1} may be related to the γ(C–H) and γ(C–C) vibrations that are usually found in polycyclic aromatic compounds of hydrocarbons [48], Fig. 1a.

FTIR spectrum of SAC after sorption of Pb^{2+}, Co^{2+}, and Cd^{2+} ions is illustrated in Fig. 1b. Some peaks are shifted after Pb^{2+}, Co^{2+}, and Cd^{2+} – loaded SAC, indicating the participation of these functional groups in the SAC binding of Pb^{2+}, Co^{2+}, and Cd^{2+} ions [14]. The broadband appears at 3,427 cm^{-1} shifted to 3,423 cm^{-1} after metal ion sorption, suggesting the participation of –OH in forming complexes with metal ions [49]. In comparison, the peak at 1,646.06 cm^{-1} disappeared after Pb^{2+}, Co^{2+}, and Cd^{2+} sorption by SAC. The C=O peak at 1,569.93 cm^{-1} gets shifted to 1,560 cm^{-1}, and the peak at 1,413.72 cm^{-1} allocated to COO– groups, shifted to 1,449.41 cm^{-1}. Additionally, the C–O appeared at 1,039.89 cm^{-1} was appeared at 1,043.45 after Pb^{2+}, Co^{2+}, and Cd^{2+} ions sorption. In contrast, the peak is seen at 702.48 cm^{-1} associated with C–O–C functional groups of esters, ether, or phenol 703.75 cm^{-1}. Likewise, the peak appears at 469.21 cm^{-1} shifted to 474.23 cm^{-1}.

Depending on the shifts as mentioned above in the bands that appeared in the FTIR spectrum of SAC adsorbent, it able be noted that some of the SAC functional groups like –OH, –C–H, –C=O, C==C and –COO– could act as active adsorption sites for the Pb^{2+}, Co^{2+}, and Cd^{2+} ions [49,50] and responsible for the metal ions binding [51]. The reduction in wavenumbers of specific bands in the FTIR spectrum after sorption Fig. 1b shows that interactions between the Pb^{2+}, Co^{2+}, and Cd^{2+} ions and those functional groups that occur during the sorption process [52]. The interactions between Pb^{2+}, Co^{2+}, and Cd^{2+} and some functional groups may be led to a shift in specific functional groups' vibrations. The coordination sites of some functional groups are changed [53].

Scanning electron microscope (SEM) was applied to identify the morphology of the surface of the SAC sample, where the image of SAC using SEM Fig. 2a indicates that the SAC surface is extremely unequal, porous and channels in

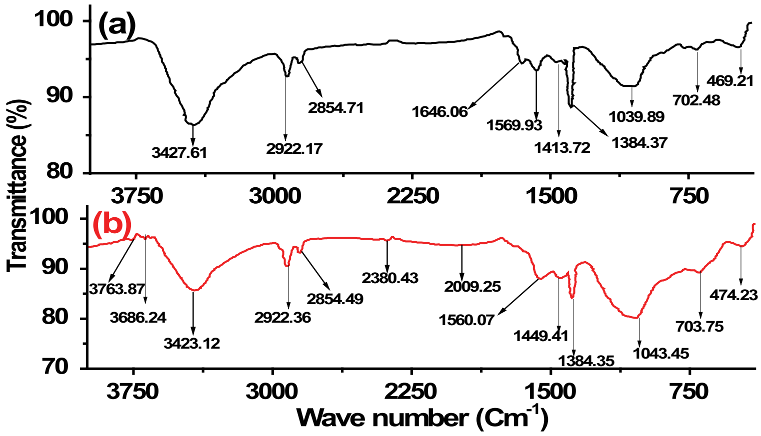

Fig. 1. FTIR spectrum of SAC: (a) SAC treated with H_3PO_4 and limestone before adsorption and (b) SAC treated with H_3PO_4 and limestone after adsorption metal ions.

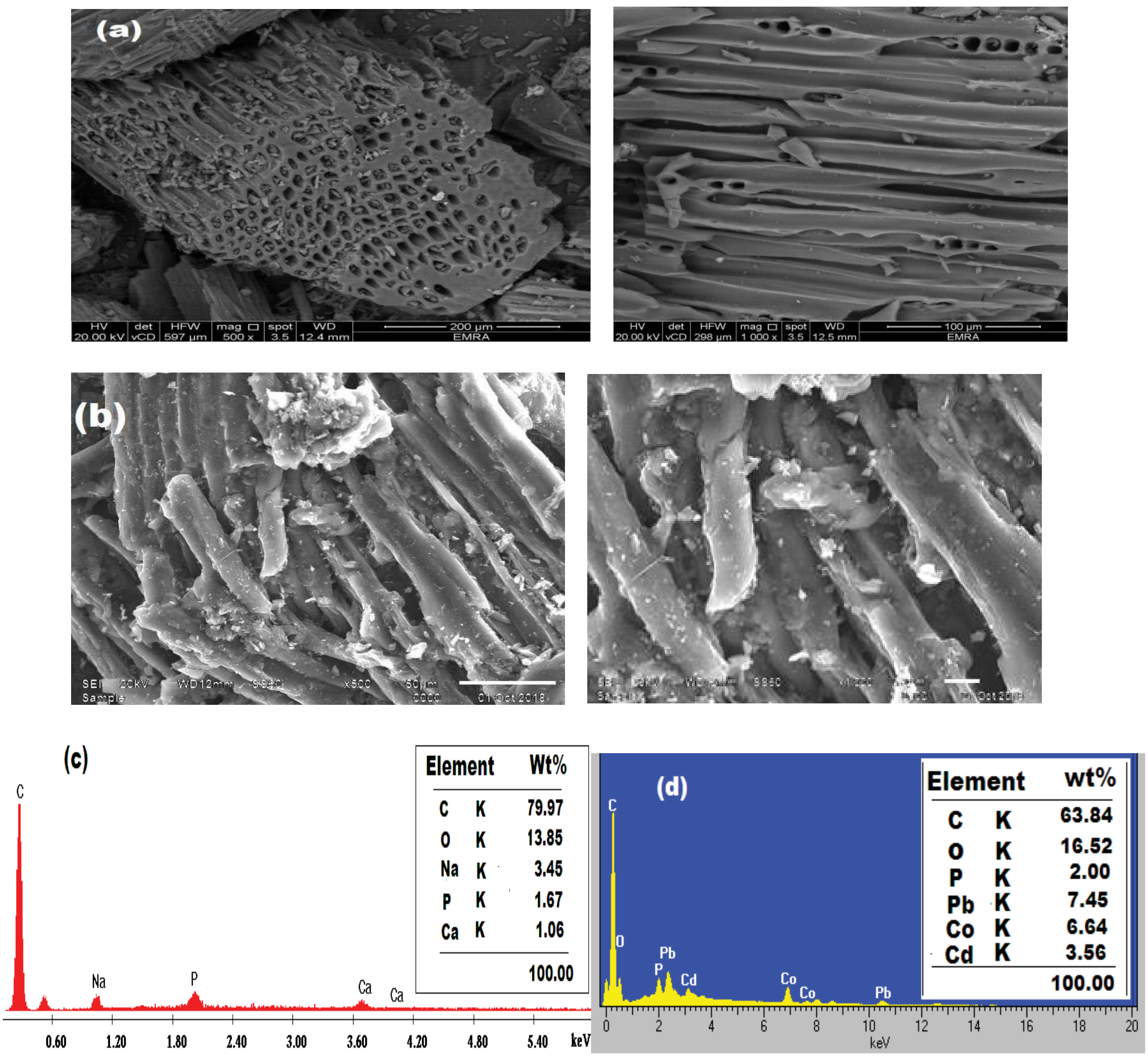

Fig. 2. SEM surface images and EDX analysis of the SAC adsorbent: (a) SEM of the SAC before sorption, (b) SEM of the SAC after sorption, (c) EDX analysis of the SAC adsorbent before adsorption, and (d) EDX analysis of the SAC adsorbent after adsorption.

the SAC structure pronounced as structures resembling a hole, and this might be due to the activation process using H_3PO_4 and CO_2 produced during calcination of limestone. Still, it can be understood clearly from Fig. 2b after sorption of Pb^{2+}, Co^{2+}, and Cd^{2+} ions, the SAC surface is wrapped with Pb^{2+}, Co^{2+}, and Cd^{2+} ions and surface anomalies.

The SAC sorbent energy-dispersive X-ray spectroscopy (EDX) analysis Fig. 2c before adsorption primarily refers to carbon (79.97 wt.%), oxygen (13.85 wt.%), and sodium (3.45 wt.%) together with phosphorus and calcium traces. Fig. 2d after adsorption indicates that the contents of carbon (63.84 wt.%), oxygen (16.52 wt.%), phosphorus (2.00 wt.%), lead (7.45 wt.%), cobalt (6.64 wt.%), and cadmium (3.56 wt.%) demonstrated the successful metal ions adsorption by the SAC adsorbent. The EDX analysis results of the SAC adsorbent before and after Pb^{2+}, Co^{2+}, and Cd^{2+} ions adsorption give credibility to the observation that the SAC adsorbent was able to remove these metal ions from their aqueous solution.

3.2. Parameters affecting the sorption process

3.2.1. Effect of pH

The pH of the aqueous solution plays a significant role in the metal ions sorption process. It is considered a critical parameter that impacts the metal ion speciation form, ionization of sorbate species, and functional groups' ionization on the sorbent surface [54]. With increasing the pH value, the adsorption of sorbate species will increase on the adsorbent's surface [55]. The metal ion sorption is considered to be reliant on the pH of the aqueous medium. It is known that heavy metals sorption is dependent on the aqueous solution's pH. The influence of pH on the sorption of Pb^{2+}, Co^{2+}, and Cd^{2+} ions with SAC from aqueous mediums was identified. The solution pH was varied from 1 to 8. It is observed that the sorption of Pb^{2+}, Co^{2+}, and Cd^{2+} ions increases in the pH range between 1 and 6, accompanied by a gradual rise in the pH value of the adsorbent being investigated. As at low pH, the repulsive force between the positive charges Pb^{2+}, Co^{2+}, and Cd^{2+} ions and sorbent increased, resulting in decreased removal efficiency [56]. Likewise, lower adsorption at acidic pH is attributable to the rivalry between H^+ ions and metal ions for the adsorbent surface adsorption sites [57]. The negativity of the sorption sites increases with the rise in pH, resulting in increased uptake of Pb^{2+}, Co^{2+}, and Cd^{2+} ions. The results showed that the extreme sorption was recorded for ions Pb^{2+}, Co^{2+}, and Cd^{2+} at pH 6, Fig.3a.

3.2.2. Effect of contact time

The impact of contact time on Pb^{2+}, Co^{2+}, and Cd^{2+} ions adsorption was investigated. The results have shown that the removal % Pb^{2+}, Co^{2+}, and Cd^{2+} ions is increased with the contact time. Likewise, the maximum sorbed quantity of Pb^{2+}, Co^{2+}, and Cd^{2+} was detected within 90 min. Subsequently, the sorption continues at a slightly slower pace until equilibrium, and the constant state was reached after equilibrium, as observed in Fig. 3b. The rapid sorption of Pb^{2+}, Co^{2+}, and Cd^{2+} ions at the initial times may also be due to the abundance of the sorbent's surface-active sites. With increasing time, the sorption process becomes slow because of the decline in the numeral of active adsorption sites on the adsorbent in addition to metal ions concentration [58]. These results are significant; since the equilibrium time is crucial for the cost-effective treatment of wastewater. The optimum contact time at which maximum sorption capacity is 90 min for metal ions.

3.2.3. Effect of concentration of metal ions

The influence of concentration of metal ions was investigated in the range of 10–400 mg/L Pb^{2+}, Co^{2+}, and Cd^{2+}. The pH value was fixed at 6 for Pb^{2+}, Co^{2+}, and Cd^{2+}. The sorption capacity of Pb^{2+}, Co^{2+}, and Cd^{2+} ions has increased by the rising metal concentration at 25°C till saturation, Fig. 3c. It was evident that the higher uptake q_e of metal ions at the low concentration can be attributed to the number of available surface-active sites of the sorbent is much greater than the number of sorbate species that can be adsorbed, and more appropriate sites became involved first. As the metal concentration increases, the sites become saturated, and the lack of available surface active sites becomes involved in the sorption process, leading to a reduction of uptake [58]. It is apparent from Fig. 3c that when higher metal ions concentration was used, the quantity sorbed on the sorbent surface at lower adsorbate concentrations was less than the equivalent amount.

3.2.4. Effect of temperature

The effect of temperature on the sorption capacity of Pb^{2+}, Co^{2+}, and Cd^{2+} in the range from 298 to 333 K was studied. The key reason for choosing this temperature range is to be suitable for surface water, groundwater, and industrial water treatment. The experimental data are given in Fig. 3d indicate that the magnitude of sorption is directly related to the solution temperature in the sorption of Pb^{2+}, Co^{2+}, and Cd^{2+}. The sorption capacity of Pb^{2+}, Co^{2+}, and Cd^{2+} was increased by increasing the temperature above room temperature. This may be attributable to the fact that the temperature will increase the sorbate diffusion rate from the solution phase to the sorbent's surface. Likewise, the rise of temperature causes the increase of the ionization of active sorption sites. Consequently, their activity increases towards the sorption Pb^{2+}, Co^{2+}, and Cd^{2+} ions from the solutions and increases metal sorbent complexes [59]. On the other hand, the increase of temperature may weaken the bond formed between the Pb^{2+}, Co^{2+}, and Cd^{2+} ions and the active surface sites of sorbent, increasing the amount of metal ions adsorbed on the sorbent surface. Hence, the temperature rise makes a great surface area for sorption at the sorbent surface [60].

3.3. Kinetics and isotherm models

3.3.1. Sorption isotherms

The sorption isotherm is utilized to explain the nature of the interaction between the sorbate and the sorbent. The most isotherms utilized are the Langmuir model [61] and Freundlich [62]. Langmuir model postulates that the sorption process occurs by forming an adsorbate monolayer

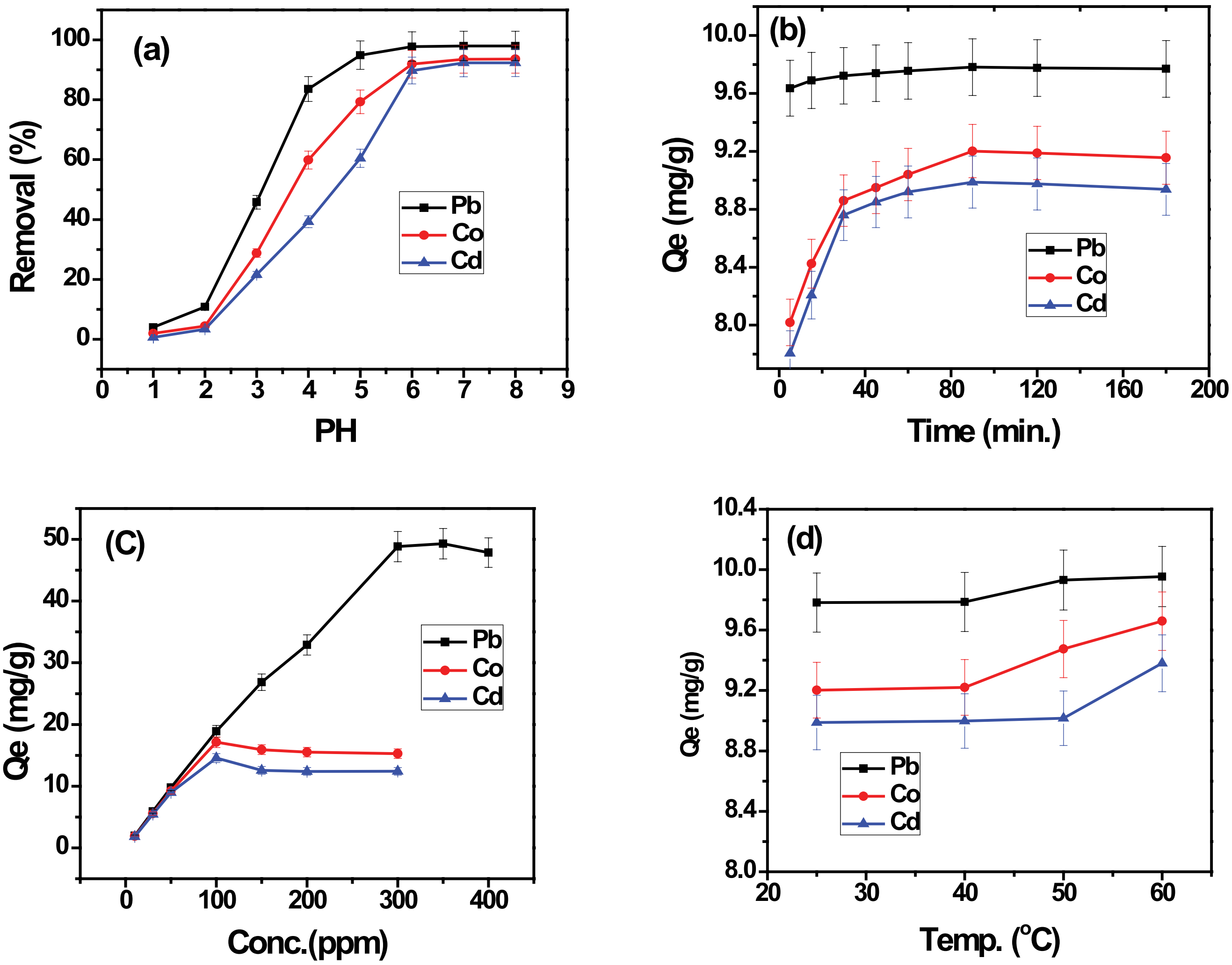

Fig. 3. Effect of sorption parameters including: (a) pH, (b) contact time, (c) concentration of metal ions, and (d) temperature.

at a definite number of active sites of sorbent [63]. The main equation of Langmuir isotherm is shown as:

$$\frac{C_e}{q_e} = \left(\frac{1}{q_m b}\right) + \left(\frac{C_e}{q_m}\right) \tag{3}$$

where C_e is the sorbate concentration in solutions at equilibrium (mg/L), q_e is equilibrium sorbate concentration on sorbent (mg/g), q_m is maximum sorption capacity of the sorbent (mg/g), b is Langmuir sorption constant (L/mg). The plot of C_e/q_e vs. C_e, as shown in Eq. (3), must be a straight line where the slope and intercept are equivalent to $1/q_m$ and $1/q_m b$, respectively, when sorption undergoes the Langmuir model.

The graphic representation of (C_e/q_e) against C_e gives a straight line for Pb^{2+}, Co^{2+}, and Cd^{2+} ions adsorbed on SAC, as shown in Fig. 4. The values of constants b and q_{max} were estimated from the graph's intercept and slope, respectively, Table 1. The value of maximum sorption capacity of the adsorbent q_{max} is corresponding to the monolayer that covers the surface of the sorbent and defines the overall sorbent capacity for particular ions.

The calculated correlation coefficients (R^2) are given in Table 1. The higher values of correlation coefficient 0.98, 0.99, and 0.99 for Pb^{2+}, Co^{2+}, and Cd^{2+}, respectively, are produced from the Langmuir isotherm. The calculated adsorption capacity (q_{max}) determined from the Langmuir model for Pb^{2+}, Co^{2+}, and Cd^{2+} was 50.65, 15.53, 12.54 mg/g, respectively, which is very close to the experimental value. The maximum value of metal sorption (q_m) for metal ions studied followed the order: $Pb^{2+} > Co^{2+} > Cd^{2+}$.

The affinity of Pb^{2+}, Co^{2+}, and Cd^{2+} to be sorbed on the SAC sorbent is represented as the constant dimensionless (R_L), defined as the intensity of sorption or separation factor and measured from Eq. (4). The value R_L refers to the sorption nature [63].

$$R_L = \frac{1}{\left(1 + bC_0\right)} \tag{4}$$

where C_0 is the highest initial sorbate concentration and b is the constant of Langmuir. Based on the values of R_L, the process of sorption is known to be irreversible

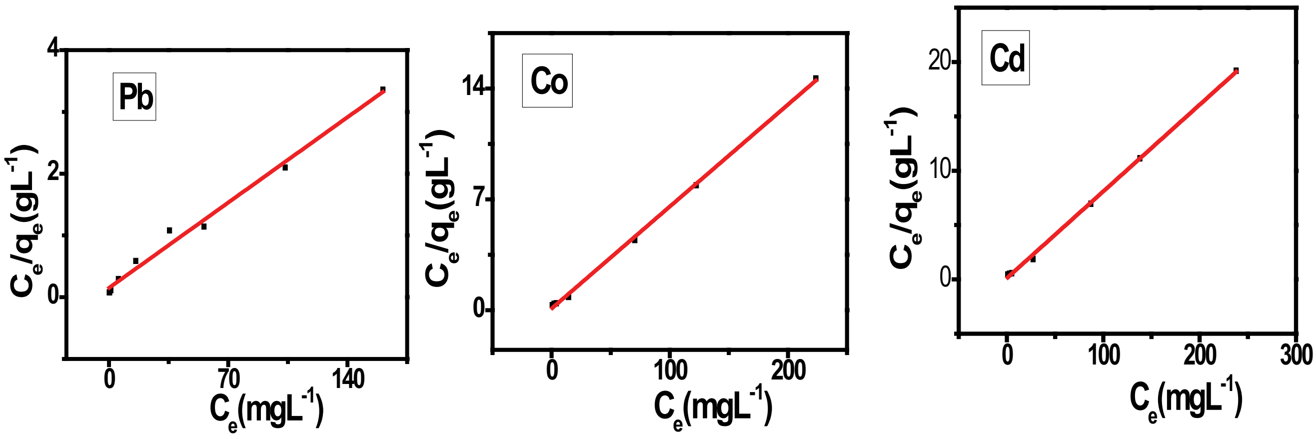

Fig. 4. Langmuir model graphs of the adsorption of Pb^{2+}, Co^{2+}, and Cd^{2+} using SAC.

Table 1
Langmuir, Freundlich and kinetic parameters for the Pb^{2+}, Co^{2+}, and Cd^{2+} adsorption using SAC activated carbon

Isotherms parameter							
Metal	$q_{e,exp.}$ (mg/g)	Langmuir isotherm			Freundlich isotherm		
		q_{max} (mg/g)	b (L/mg)	R^2	n	K (mg/g)	R^2
Pb	**48.83**	**50.65**	0.13	**0.98**	3.6	8.83	**0.67**
Co	**15.51**	**15.53**	0.58	**0.99**	3.19	4.02	**0.68**
Cd	**12.39**	**12.54**	0.66	**0.99**	3.48	3.53	**0.65**
Kinetic parameters							
Metal	C_0 (mg/L)	$q_{e,exp.}$ (mg/g)		$q_{e,cal.}$ (mg/g)		K_1 (min^{-1})	R^2
Pseudo-first-order							
Pb		9.78		0.16		0.030	0.98
Co	50	9.20		1.29		0.036	0.96
Cd		8.99		1.49		0.053	0.97
Pseudo-second-order							
Pb		**9.78**		**9.77**		1.08	**1**
Co	50	**9.20**		**9.17**		0.107	**0.99**
Cd		**8.99**		**9.08**		0.093	**0.99**

($R_L = 0$), favorable ($0 < R_L < 1$), linear sorption ($R_L = 1$), and unfavorable ($R_L > 1$) [63].

The calculated values of R_L in the present investigation were found to between 0.018–0.43, 0.005–0.14, and 0.005–0.13 for Pb^{2+}, Co^{2+}, and Cd^{2+}, respectively; confirming the favorable adsorption of Pb^{2+}, Co^{2+} and Cd^{2+}.

The isotherm of Freundlich postulates multilayer sorption at active hetero-energetic sites. Freundlich's linear equation may be written as [64]:

$$\log q_e = \log K_f + \frac{1}{n}\log C_e \quad (5)$$

where K_f (mg g^{-1}) and n are the adsorption capacity and adsorption intensity constants, respectively. K_f values may be utilized to describe the comparative sorption capacity, and if $1/n$ values are between 0.1 and 1, this refers to better sorption on the adsorbent [63].

The Freundlich isotherm sorption validity was evaluated through drawing logq_e vs. logC_e, giving linear relationships as shown in Fig. 5. According to the values of R^2 and adsorption capacity (q_{max}) values, it may be assumed that the Langmuir isotherm is better suited to the experimental results than the Freundlich isotherm.

3.3.2. Adsorption kinetic studies

First and second-order kinetic models have been used for the analysis of sorption kinetic data. For the analysis of sorption kinetics, experimental results were implemented to first and second-order kinetic models [65]. Lagergren's first-order model equation is among the most commonly used for liquid sorption studies and is expressed by Eq. (6).

$$\log\left(q_e - q_t\right) = \log q_e - \frac{K_f}{2.303}t \quad (6)$$

where q_t and q_e are the sorbed solute quantities (mg/g) at time t (min) and equilibrium, respectively. K_f is a pseudo-first-order constant (min^{-1}). By plot log($q_e - q_t$) against (t), which gives a straight line illustrated in Fig. 6a, q_e (mg g^{-1}) value can be generated from the intercept and the K_f (min^{-1}) value from the slope, Table 1.

Table 1 shows that the values of (R^2) are low and the q_e values calculated from the graph plotted don't confirm the experimental results. This ensures that the sorption of Pb^{2+}, Co^{2+}, and Cd^{2+} onto SAC doesn't obey first-order kinetics.

Whereas Eq. (7) represents the linear shape of the second-order model equation. This equation was developed by Ho and McKay [66].

$$\frac{t}{q_t} = \frac{1}{K_s q_e^2} + \frac{t}{q_e} \quad (7)$$

where q_e is the quantity of solute sorbed (mg/g) at the equilibrium while q_t is the quantity of solute sorbed (mg/g) at t

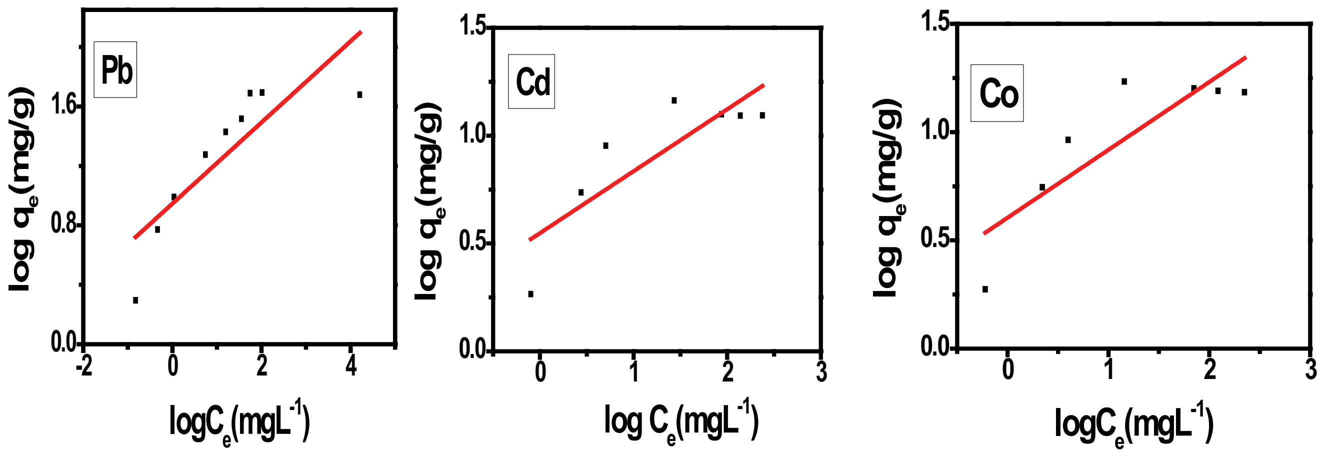

Fig. 5. Freundlich model graphs of the sorption of Pb^{2+}, Co^{2+}, and Cd^{2+} using SAC.

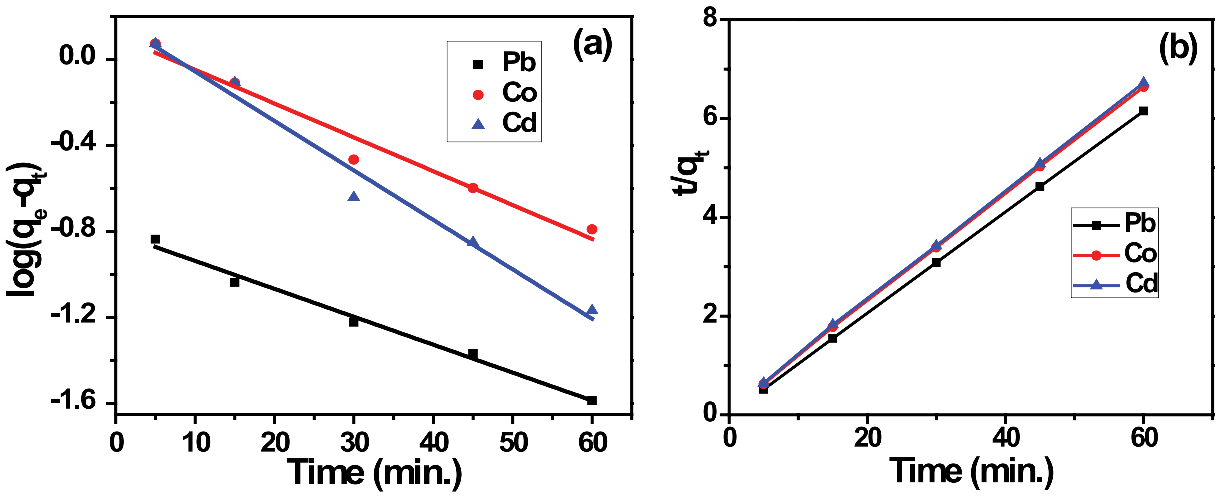

Fig. 6. Kinetic sorption models for Pb^{2+}, Co^{2+}, and Cd^{2+} on SAC carbon (a) first-order model and (b) second-order model.

(min). K_s is the equilibrium constant of the pseudo-second-order rate (g/mg min). Plotting t/q_t against (t), which gives a straight line illustrated in Fig. 6b, the values of K_s and q_e can be estimated from the intercept and the slope, respectively, Table 1.

The value of q_e derived from the second-order model along with correlation coefficient R^2, Table 1, indicated that the values of q_e are consistent with the experimental results. The R^2 of the second-order kinetic model was greater than that of the first-order kinetic model for Pb^{2+}, Co^{2+}, and Cd^{2+} signifying that the pseudo-second-order is better fitted than the pseudo-first-order model and implies that the sorption completely conforms to second-order reaction. Consequently, the sorption process for Pb^{2+}, Co^{2+}, and Cd^{2+} seemed to be dominated by a chemisorption mechanism [67].

3.4. Thermodynamic parameters

The sorption process is highly reliant upon the system's operating temperature [63]. Sorption experiments of Pb^{2+}, Co^{2+} and Cd^{2+} are carried out using pH 6 solutions at different four temperatures of 298, 313, 323 and 333 K. The following equations were used to measure thermodynamic parameters like free adsorption energy ($\Delta G°$), adsorption heat ($\Delta H°$) and standard entropy ($\Delta S°$) as a function of temperature during the adsorption process using the initial concentration of 50 mg/L for Pb^{2+}, Co^{2+}, and Cd^{2+} ions and sorbent dose of 0.25 g/50 mL of SAC.

$$\Delta G° = -RT\ln K_c \quad (8)$$

$$\Delta G° = \Delta H° - T\Delta S° \quad (9)$$

$$\ln K_c = \frac{\Delta S°}{R} - \frac{\Delta H°}{RT} \quad (10)$$

The values of $\Delta S°$ and $\Delta H°$ were derived from the intercept and slope of the linear graph of $\ln K_c$ against $1/T$ shown in Fig. 7 and given in Table 2.

Positive values of $\Delta H°$ indicated the endothermic nature of sorption, which has also been demonstrated by the rise in Pb^{2+}, Co^{2+}, and Cd^{2+} sorption capacity of the adsorbent with temperature rise values. The negative values of $\Delta G°$ refer to the procedure's visibility, and the Pb^{2+},

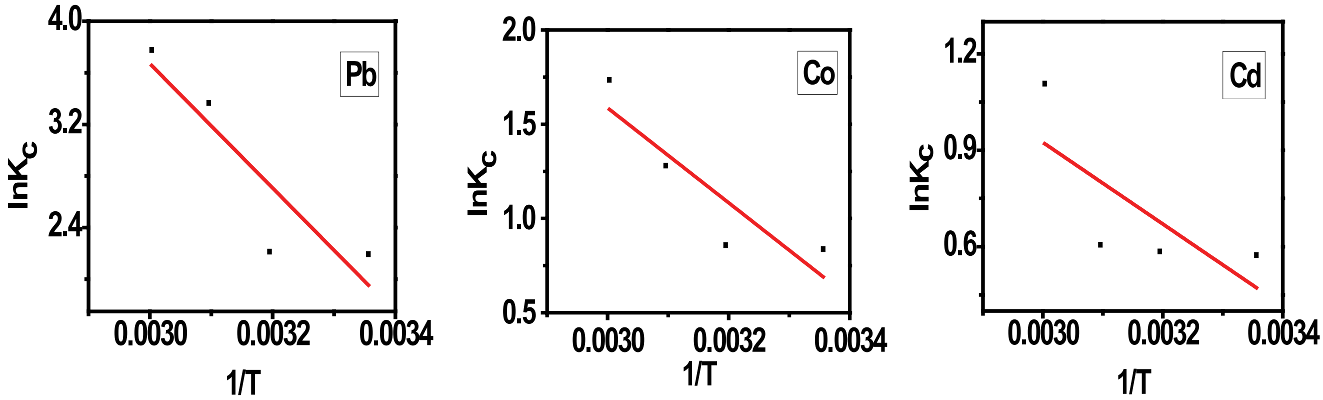

Fig. 7. Graph lnK_c against $1/T$ for Pb^{2+}, Co^{2+}, and Cd^{2+} sorption to SAC.

Table 2
Thermodynamic parameters of Pb^{2+}, Co^{2+}, and Cd^{2+} adsorption on SAC

Metal	$\Delta G°$ (kJ/mol)				$\Delta H°$ (kJ/mol)	$\Delta S°$ (J/mol/K)
	298 K	313 K	323 K	333 K		
Pb	–4.85	–7.10	–8.62	–10.12	**40.08**	**150.76**
Co	–1.71	–2.85	–3.60	–4.37	**20.92**	**75.95**
Cd	–1.17	–1.76	–2.15	–2.54	**10.55**	**39.35**

Co^{2+}, and Cd^{2+} adsorption on SAC adsorbent were spontaneous [57,63]. The more negative values obtained for $\Delta G°$ with rising temperature express the sorption process is more favorable at a higher temperature. Positive $\Delta S°$ values show an increase in the level of the sorbed ions' freedom. The rise of sorption at extreme temperatures could be related to the extension of pore size and/or the adsorbent surface activation [68].

3.5. Desorption and regeneration studies

Recovery and consequent recycling of sorbent are of vital significance for the effective applications of any sorbent. The effective regeneration must recover the sorbent almost to its original shape for successful recycling without reducing contaminants sorption capacity and without any physical changes or damages [69]. Furthermore, the regeneration process's objective is to re-use the same sorbent for the for heavy metals' sorption, which should decrease the cost of the treatment process. Recovery of the Pb^{2+}, Co^{2+}, and Cd^{2+} ions was carried out by various desorbing agents containing mineral acids as H_2SO_4, HNO_3, HCl, NaOH, and Na_2CO_3. These desorbing agents may change the sorbed ions' chemical shape and/or break the bond between sorbate and adsorbents.

Results revealed that the adsorption process's reversibility is only nearly complete in the case of HCl and HNO_3 for Pb^{2+}, Co^{2+}, and Cd^{2+}. In this concern, various concentrations of HCl and HNO_3 were tested. The maximum recovery of Pb^{2+} was obtained using 0.5 M HCl and 0.5 HNO_3 with elution efficiencies of 99.7% and 63.5%, respectively. In comparison, the ultimate recovery of Co^{2+} was achieved using 1.0 M HCl and 1.0 HNO_3 with elution efficiencies of 98.8% and 98.3%, respectively. The full recovery of Cd^{2+} was performed using 0.5 M HCl and 0.5 HNO_3 with elution efficiencies of 97.7% and 85%, respectively.

3.6. Comparative to other sorbents

To explain SAC's validity as an efficient sorbent for Pb^{2+}, Co^{2+}, and Cd^{2+}, its sorption capacity must be evaluated by comparing other sorbents mentioned. The q_{max} values for sorption Pb^{2+}, Co^{2+}, and Cd^{2+} on different sorbents are compared with our sorbent and are summarized in Table 3. The uptake achieved is comparable with other reported sorbents applied to remove Pb^{2+}, Co^{2+}, and Cd^{2+} from aqueous solutions. The results indicated that SAC sorbent could be regarded as an auspicious material for eliminating Pb^{2+}, Co^{2+}, and Cd^{2+} ions.

3.7. Application study

In addition to the previous results and the proven ability of prepared SAC activated carbon produced from agricultural biomass to remove metal ions, its ability to treat the surface water and groundwater containing metal ions was studied. Moreover, studying the possibility to treat industrial wastewater (methylene blue and congo red) and disinfection by-products (DBP's), which is called trihalomethanes (THMs), which represent one of the most dangerous problems results during disinfection of water by chlorine in water plants. Removal of Pb^{2+}, Co^{2+}, and Cd^{2+} from 50 mL surface and groundwater samples containing different concentrations (50 and 100 ppm) and a sorbent dose of 0.250 g at 90 min contact time was found to be effective in removing Pb^{2+}, Co^{2+}, and Cd^{2+}. This experiment was performed in five cycles, and a reasonable degree of sorption was achieved. Fig. 8 shows that SAC has shown good ability to treat Pb^{2+}, Co^{2+}, and Cd^{2+} ions at different concentrations (50 and 100 ppm) in surface and groundwater. In general, the ability of SAC to remove metal ions in the surface water is higher than that of groundwater. Moreover, the order of percent removal of metal ions was $Pb^{2+} > Co^{2+} > Cd^{2+}$. The obtained results revealed a high affinity for sorption removal of methylene blue and a low tendency to sorption congo red using the prepared SAC, as

Table 3
Comparison of maximum adsorption capacities of Pb^{2+}, Co^{2+}, and Cd^{2+} on various sorbents

Adsorbents	Sorption capacity (mg/g)			References
	Pb	Co	Cd	
Pineapple fruit peel	28.55	–	42.10	[70]
Modified rice straw	9.42	–	9.7	[71]
Bamboo activated carbon	5.09	–	7.843	[72]
Corn cob	20	2.52	10.31	[73]
Chitin with polypyrrole	8.64	–	6.17	[74]
Commercial activated carbon	20.30	–	27.30	[50]
Raw cherry kernels	10.84	–	11.23	[75]
Peat moss	–	30.03	–	[12]
Spent green tea leaves	–	7.09	–	[76]
Palygorskite	–	8.88	–	[13]
Sawdust activated with H_3PO_4 and limestone	50.65	15.53	12.54	Present study

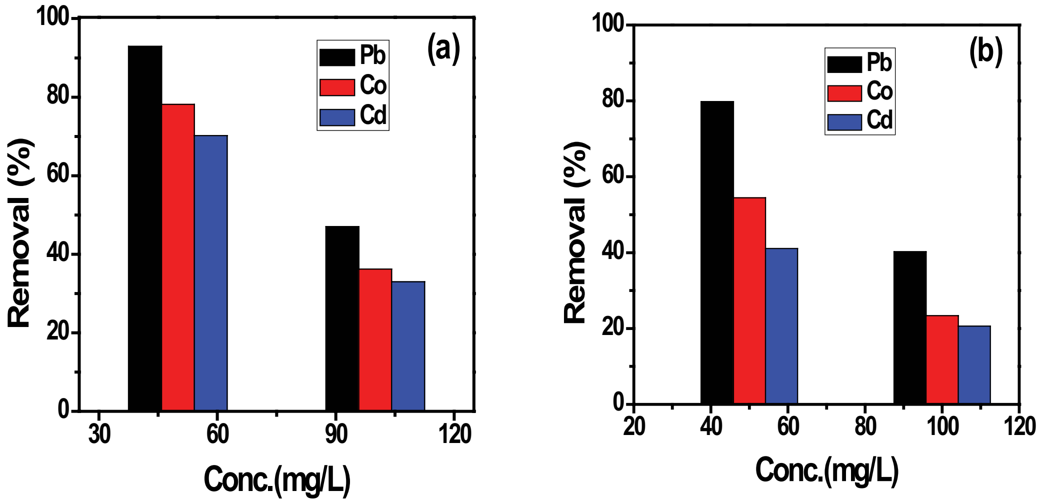

Fig. 8. Evaluation of sorptive removal of Pb^{2+}, Co^{2+}, and Cd^{2+} by SAC from surface and groundwater: (a) % removal of from surface water and (b) % removal from groundwater.

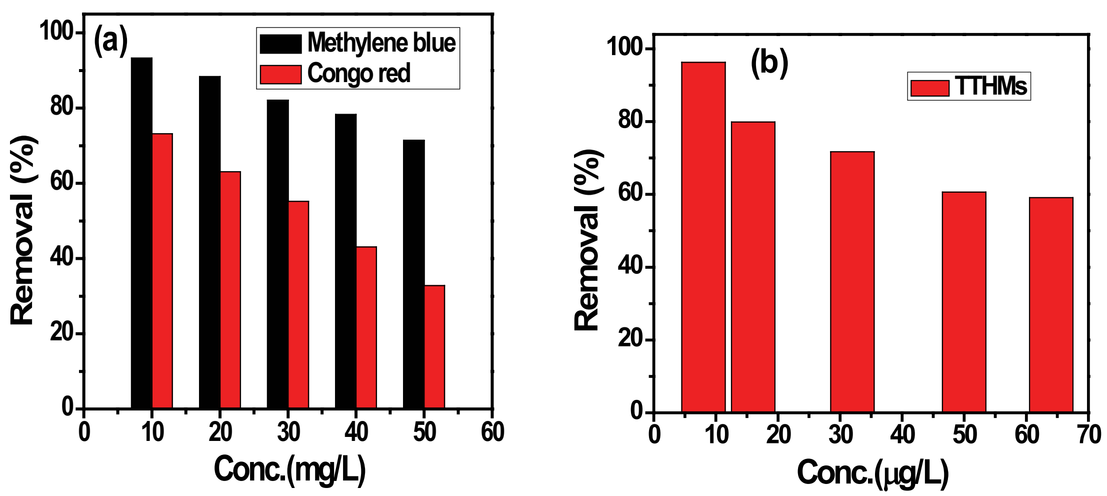

Fig. 9. Evaluation of sorptive removal of some organic pollutants by SAC: (a) % removal of methylene blue and congo red and (b) % removal of THMs.

shown in Fig. 9a. Likewise, the results indicated that SAC had been a successfully applied material for the removal THMs from aqueous solutions at a different standard mixture of THMs (8, 16, 32, 50, and 64 μg/L) as shown in Fig. 9b. Therefore, SAC proves a good ability to remove DBP's from drinking water, especially THMs.

4. Conclusions

The present study indicated that activated carbon prepared from sawdust obtained from the local timber industry workshop has successfully removed Pb^{2+}, Co^{2+}, and Cd^{2+} ions from aqueous solutions. The EDX analysis results of the SAC adsorbent before and after Pb^{2+}, Co^{2+}, and Cd^{2+} ions adsorption showed the presence of the three metal ions on the sorbent surface. They confirmed the observation that the SAC sorbent was able to remove these metal ions from their aqueous solutions. The efficiency of SAC was investigated using a batch adsorption technique under various experimental conditions. The maximum sorption was observed at pH 6 within 90 min. The equilibrium sorption data fit better with the Langmuir equation than Freundlich. A pseudo-second-order model sufficiently describes the kinetics of the adsorption process. The estimated thermodynamic parameters showed the expediency, endothermic and spontaneous nature of the sorption process. Moreover, the efficacy of SAC in the treatment of metal ions from surface and groundwater and other organic pollutants has been applied. The results revealed that SAC had been successfully applied and effective material for treating of heavy metals and some organic pollutants.

References

[1] N.B. Singh, G. Nagpal, S. Agrawal, Rachna, Water purification by using adsorbents: a review, Environ. Technol. Innovation, 11 (2018) 187–240.

[2] T.S. Anirudhan, S.S. Sreekumari, Adsorptive removal of heavy metal ions from industrial effluents using activated carbon derived from waste coconut buttons, J. Environ. Sci., 23 (2011) 1989–1998.

[3] L. Xiong, C. Chen, Q. Chen, J. Ni, Adsorption of Pb(II) and Cd(II) from aqueous solutions using titanate nanotubes prepared via hydrothermal method, J. Hazard. Mater., 189 (2011) 741–748.

[4] R. Karthik, S. Meenakshi, Removal of Pb(II) and Cd(II) ions from aqueous solution using polyaniline grafted chitosan, Chem. Eng. J., 263 (2015) 168–177.

[5] Z. Khademi, B. Ramavandi, M.T. Ghaneian, The behaviors and characteristics of a mesoporous activated carbon prepared from *Tamarix hispida* for Zn(II) adsorption from wastewater, J. Environ. Chem. Eng., 3 (2015) 2057–2067.

[6] A. Rahbar, S. Farjadfard, M. Leili, R. Kafaei, V. Haghshenas, B. Ramavandi, Experimental data of biomaterial derived from *Malva sylvestris* and charcoal tablet powder for Hg^{2+} removal from aqueous solutions, Data Brief, 8 (2016) 132–135.

[7] N. Kataria, V.K. Garg, Green synthesis of Fe_3O_4 nanoparticles loaded sawdust carbon for cadmium(II) removal from water: regeneration and mechanism, Chemosphere, 208 (2018) 818–828.

[8] A. Bhatnagar, M. Sillanpää, Removal of natural organic matter (NOM) and its constituents from water by adsorption – a review, Chemosphere, 166 (2017) 497–510.

[9] E. Borai, M. Attallah, R. Koivula, A. Paajanen, R. Harjula, Separation of europium from cobalt using antimony silicates in sulfate acidic media, Miner. Process. Extr. Metall. Rev., 33 (2012) 204–219.

[10] G. Gentscheva, P. Vassileva, P. Tzvetkova, L. Lakov, O. Peshev, E. Ivanova, Activated carbon sorbent with thioetheric sites-preparation and characterization, J. Porous Mater., 15 (2008) 331–334.

[11] B.H. Hameed, A.L. Ahmad, K.N.A. Latiff, Adsorption of basic dye (methylene blue) onto activated carbon prepared from rattan sawdust, Dyes Pigm., 75 (2007) 143–149.

[12] C. Caramalău, L. Bulgariu, M. Macoveanu, Cobalt(II) removal from aqueous solutions by adsorption on modified peat moss, Chem. Bull. "POLITEHNICA" Univ. (Timişoara), 54 (2009) 13–17.

[13] M. He, Y. Zhu, Y. Yang, B. Han, Y. Zhang, Adsorption of cobalt(II) ions from aqueous solutions by palygorskite, Appl. Clay Sci., 54 (2011) 292–296.

[14] M.N.M. Ibrahim, W.S.W. Ngah, M.S. Norliyana, W.R. Wan Daud, M. Rafatullah, O. Sulaiman, R. Hashim, A novel agricultural waste adsorbent for the removal of lead(II) ions from aqueous solutions, J. Hazard. Mater., 182 (2010) 377–385.

[15] S. Dowlatshahi, A.R.H. Torbati, M. Loloei, Adsorption of copper, lead and cadmium from aqueous solutions by activated carbon prepared from saffron leaves, Environ. Health Eng. Manage. J., 1 (2014) 37–44.

[16] T. Bohli, A. Ouederni, N. Fiol, I. Villaescusa, Uptake of Cd^{2+} and Ni^{2+} metal ions from aqueous solutions by activated carbons derived from waste olive stones, Int. J. Chem. Eng. Appl., 3 (2012) 232–236.

[17] A. Almasi, M. Omidi, M. Khodadadian, R. Khamutian, M.B. Gholivand, Lead(II) and cadmium(II) removal from aqueous solution using processed walnut shell: kinetic and equilibrium study, Toxicol. Environ. Chem., 94 (2012) 660–671.

[18] B.G.N. Sewwandi, M. Vithanage, S.S.R.M.D.H.R. Wijesekara, M.I.M. Mowjood, S. Hamamoto, K. Kawamoto, Adsorption of Cd(II) and Pb(II) onto humic acid-treated coconut (*Cocos nucifera*) husk, J. Hazard. Toxic Radioact. Waste, 18 (2014) 1–10.

[19] Z. Zhou, Z. Xu, Q. Feng, D. Yao, J. Yu, D. Wang, S. Lv, Y. Liu, N. Zhou, M.-E. Zhong, Effect of pyrolysis condition on the adsorption mechanism of lead, cadmium and copper on tobacco stem biochar, J. Cleaner Prod., 187 (2018) 996–1005.

[20] B.G. Alhogbi, Potential of coffee husk biomass waste for the adsorption of Pb(II) ion from aqueous solutions, Sustainable Chem. Pharm., 6 (2017) 21–25.

[21] S.H. Siddiqui, R. Ahmad, Pistachio Shell Carbon (PSC) – an agricultural adsorbent for the removal of Pb(II) from aqueous solution, Groundwater Sustainable Dev., 4 (2016) 42–48.

[22] H. Peng, P. Gao, G. Chu, B. Pan, J. Peng, B. Xing, Enhanced adsorption of Cu(II) and Cd(II) by phosphoric acid-modified biochars, Environ. Pollut., 229 (2017) 846–853.

[23] A. Abdolali, W.S. Guo, H.H. Ngo, S.S. Chen, N.C. Nguyen, K.L. Tung, Typical lignocellulosic wastes and by-products for biosorption process in water and wastewater treatment: a critical review, Bioresour. Technol., 160 (2014) 57–66.

[24] M. Rafatullah, O. Sulaiman, R. Hashim, A. Ahmad, Removal of cadmium(II) from aqueous solutions by adsorption using meranti wood, Wood Sci. Technol., 46 (2012) 221–241.

[25] R. Ouafi, Z. Rais, M. Taleb, M. Benabbou, M. Asri, Chapter 4 – Sawdust in the Treatment of Heavy Metals-Contaminated Wastewater, E. Stefan, K. Olaf, Eds., Sawdust: Properties, Potential Uses and Hazards, Nova Science Publishers, New York, NY, USA, 2017, pp. 145–182.

[26] H.A. Alalwan, M.A. Kadhom, A.H. Alminshid, Removal of heavy metals from wastewater using agricultural byproducts, J. Water Supply Res. Technol. AQUA, 69 (2020) 99–112.

[27] J. Pallarés, A. González-Cencerrado, I. Arauzo, Production and characterization of activated carbon from barley straw by physical activation with carbon dioxide and steam, Biomass Bioenergy, 115 (2018) 64–73.

[28] M. Kiliç, E. Apaydin-Varol, A.E. Pütün, Preparation and surface characterization of activated carbons from *Euphorbia rigida* by chemical activation with $ZnCl_2$, K_2CO_3, NaOH and H_3PO_4, Appl. Surf. Sci., 261 (2012) 247–254.

[29] P. Nowicki, P. Skibiszewska, R. Pietrzak, Hydrogen sulphide removal on carbonaceous adsorbents prepared from coffee industry waste materials, Chem. Eng. J., 248 (2014) 208–215.

[30] K.S.K. Reddy, A. Al Shoaibi, C. Srinivasakannan, A comparison of microstructure and adsorption characteristics of activated carbons by CO_2 and H_3PO_4 activation from date palm pits, New Carbon Mater., 27 (2012) 344–351.
[31] J.S. Cha, S.H. Park, S.-C. Jung, C. Ryu, J.-K. Jeon, M.-C. Shin, Y.-K. Park, Production and utilization of biochar: a review, J. Ind. Eng. Chem., 40 (2016) 1–15.
[32] S. Manocha, F. Ponchon, Management of lime in steel, Metals, 8 (2018) 686–701.
[33] J.M. Valverde, P.E. Sanchez-Jimenez, L.A. Perez-Maqueda, Limestone calcination nearby equilibrium: kinetics, CaO crystal structure, sintering and reactivity, J. Phys. Chem. C, 119 (2015) 1623–1641.
[34] J. Kanagaraj, T. Senthilvelan, R.C. Panda, S. Kavitha, Eco-friendly waste management strategies for greener environment towards sustainable development in leather industry: a comprehensive review, J. Cleaner Prod., 89 (2015) 1–17.
[35] S. Chaudhary, J. Iqbal, M. Hussain, Effectiveness of different fungicides and antibiotics against bacterial leaf blight in rice, J. Agric. Res., 50 (2012)109–117.
[36] T. Olinic, E. Olinic, The effect of quicklime stabilization on soil properties, Agric. Agric. Sci. Procedia, 10 (2016) 444–451.
[37] A.A. El-gray, F.B.M. Ahmed, Determination of major oxides percentages in portland cement of some sudanese cement manufactories, Am. J. Appl. Chem., 4 (2016) 14–17.
[38] C. Wang, L. Chen, L. Jia, Y. Tan, Simultaneous calcination and sulfation of limestone in CFBB, Appl. Energy, 155 (2015) 478–484.
[39] B. Xu, L. Peng, G. Wang, G. Cao, F. Wu, Easy synthesis of mesoporous carbon using nano-$CaCO_3$ as template, Carbon, 48 (2010) 2377–2380.
[40] L. Kong, M. Su, Y. Peng, L. Hou, J. Liu, H. Li, Z. Diao, K. Shih, Y. Xiong, D. Chen, Producing sawdust derived activated carbon by co-calcinations with limestone for enhanced Acid Orange II adsorption, J. Cleaner Prod., 168 (2019) 22–29.
[41] F. Zhao, E. Repo, Y. Song, D. Yin, S.B. Hammouda, L. Chen, S. Kalliola, J. Tang, K.C. Tam, M Sillanpää, Polyethylenimine-cross-linked cellulose nanocrystals for highly efficient recovery of rare earth elements from water and a mechanism study, Green Chem., 19 (2017) 4816–4828.
[42] W. Gan, L. Gao, X. Zhan, J. Li, Preparation of thiol-functionalized magnetic sawdust composites as an adsorbent to remove heavy metal ions, RSC Adv., 6 (2016) 37600–37609.
[43] M. Can, E. Bulut, M. Özacar, Synthesis and characterization of gallic acid resin and its interaction with palladium(II), rhodium(III) chloro complexes, Ind. Eng. Chem. Res., 51 (2012) 6052–6063.
[44] C.S.T. Araújo, I.L.S. Almeida, H.C. Rezende, S.M.L.O. Marcionilio, J.J.L. Léon, T.N. de Matos, Elucidation of mechanism involved in adsorption of Pb(II) onto lobeira fruit (*Solanum lycocarpum*) using Langmuir, Freundlich and Temkin isotherms, Microchem. J., 137 (2018) 348–354.
[45] M. Moyo, L. Chikazaza, B.C. Nyamunda, U. Guyo, Adsorption batch studies on the removal of Pb(II) using maize tassel based activated carbon, J. Chem., 2013 (2013) 1–8.
[46] U. Garg, M.P. Kaur, G.K. Jawa, G. Sud, V.K. Garg, Removal of cadmium(II) from aqueous solutions by adsorption on agricultural waste biomass, J. Hazard. Mater., 154 (2008) 1149–1157.
[47] T.M. Alslaibi, I. Abustan, A. Ahmad, A. Abu Foul, Comparison of activated carbon prepared from olive stones by microwave and conventional heating for iron(II), lead(II), and copper(II) removal from synthetic wastewater, Environ. Prog. Sustainable Energy, 33 (2013) 1074–1085.
[48] D.M. Agudelo-Castañeda, E.C. Teixeira, I.L. Schneider, S.B.A. Rolim, N. Balzaretti, G.S.E. Silva, Comparison of emissivity, transmittance, and reflectance infrared spectra of polycyclic aromatic hydrocarbons with those of atmospheric particulates (PM1), Aerosol Air Qual. Res., 15 (2015) 1627–1639.
[49] M.H.M.A. Kamal, W.M.K.W.K. Azira, M. Kasmawati, Z. Haslizaidi, W.N.W. Saime, Sequestration of toxic Pb(II) ions by chemically treated rubber (*Hevea brasiliensis*) leaf powder, J. Environ. Sci., 22 (2010) 248–256.
[50] E. Asuquo, A. Martin, P. Nzerem, Adsorption of Cd(II) and Pb(II) ions from aqueous solutions using mesoporous activated carbon adsorbent: equilibrium, kinetics and characterisation studies, J. Environ. Chem. Eng., 5 (2017) 679–698.
[51] P. Chand, Y.P. Pakade, Removal of Pb from water by adsorption on apple pomace: equilibrium, kinetics, and thermodynamics studies, J. Chem., 2013 (2013) 164575, doi: 10.1155/2013/164575.
[52] C. Paduraru, L. Tofan, C. Teodosiu, Biosorption of zinc(II) on rapeseed waste: equilibrium studies and thermogravimetric investigations, Process Saf. Environ. Prot., 94 (2015) 18–28.
[53] M. Thirumavalavan, Y.L. Lai, J.F. Lee, Fourier transform infrared spectroscopic analysis of fruit peels before and after the adsorption of heavy metal ions from aqueous solution, J. Chem. Eng. Data, 56 (2011) 2249–2255.
[54] A.M. Georgescu, F. Nardou, V. Zichil, I.D. Nistor, Adsorption of lead(II) ions from aqueous solutions onto Cr-pillared clays, Appl. Clay Sci., 152 (2018) 44–50.
[55] B. Huang, Z. Li, J. Huang, L. Guo, X. Nie, Y. Wang, Y. Zhang, G. Zeng, Adsorption characteristics of Cu and Zn onto various size fractions of aggregates from red paddy soil, J. Hazard. Mater., 264 (2014) 176–183.
[56] X.Yang, G. Xu, H. Yu, Removal of lead from aqueous solutions by ferric activated sludge-based adsorbent derived from biological sludge, Arabian J. Chem., 12 (2019) 4142–4149.
[57] H.S. Hassan, M.F. Attallah, S.M. Yakout, Sorption characteristics of an economical sorbent material used for removal radioisotopes of cesium and europium, J. Radioanal. Nucl. Chem., 286 (2010) 17–26.
[58] M. Ghasemi, M. Naushad, N. Ghasemi, Y. Khosravi-fard, Adsorption of Pb(II) from aqueous solution using new adsorbents prepared from agricultural waste: adsorption isotherm and kinetic studies, J. Ind. Eng. Chem., 20 (2014) 2193–2199.
[59] M.A. Badawi, N.A. Negm, M.T.H. Abou Kana, Adsorption of aluminum and lead from wastewater by chitosan-tannic acid modified biopolymers: isotherms, kinetics, thermodynamics and process mechanism, Int. J. Biol. Macromol., 99 (2017) 465–476.
[60] P.C. Okafor, P.U. Okon, E.F. Daniel, E.E. Ebenso, Adsorption capacity of coconut (*Cocos nucifera* L.) shell for lead, copper, cadmium and arsenic from aqueous solutions, Int. J. Electrochem. Sci., 7 (2012) 12354–12369.
[61] E.H. Borai, M.F. Attallah, A.H. Elgazzar, A.S. El-Tabl, Isotherm and kinetic sorption of some lanthanides and iron from aqueous solution by aluminum silicotitante exchanger, Part. Sci. Technol., 37 (2019) 410–422.
[62] H.E. Rizk, M.F. Attallah, A.M.I. Ali, Investigations on sorption performance of some radionuclides, heavy metals and lanthanides using mesoporous adsorbent material, J. Radioanal. Nucl. Chem., 314 (2017) 2475–2487.
[63] M.F. Attallah, A.I. Abd-Elhamid, I.M. Ahmed, H.F. Aly, Possible use of synthesized nano silica functionalized by Prussian blue as sorbent for removal of certain radionuclides from liquid radioactive waste, J. Mol. Liq., 261 (2018) 379–386.
[64] D.M. Imam, S.I. Moussa, M.F. Attallah, Sorption behavior of some radionuclides using prepared adsorbent of hydroxyapatite from biomass waste material, J. Radioanal. Nucl. Chem., 319 (2019) 997–1012.
[65] M.F. Attallah, H.S. Hassan, M.A. Youssef, Synthesis and sorption potential study of Al_2O_3-ZrO_2-CeO_2 composite material for removal of some radionuclides from radioactive waste effluent, Appl. Radiat. Isot., 147 (2019) 40–47.
[66] Y-S. Ho, G. McKay, The kinetics of sorption of divalent metal ions onto sphagnum moss peat, Water Res., 34 (2000) 735–742.
[67] J. Yu, R. Chi, Y. Zhang, Z. Xu, C. Xiao, J. Guo, A situ co-precipitation method to prepare magnetic PMDA modified sugarcane bagasse and its application for competitive adsorption of methylene blue and basic magenta, Bioresour. Technol., 110 (2012) 160–166.
[68] R. Najam, S.M.A. Andrabi, Adsorption capability of sawdust of *Populus alba* for Pb(II), Zn(II) and Cd(II) ions from aqueous solution, Desal. Water Treat., 57 (2016) 29019–29035.

[69] K. Vijayaraghavan, H.Y.N. Winnie, R. Balasubramanian, Biosorption characteristics of crab shell particles for the removal of manganese(II) and zinc(II) from aqueous solutions, Desalination, 266 (2011) 195–200.
[70] A. Ahmad, A. Khatoon, S.-H. Mohd-Setapar, R. Kumarb, M. Rafatullah, Chemically oxidized pineapple fruit peel for the biosorption of heavy metals from aqueous solutions, Desal. Water Treat., 57 (2016) 6432–6442.
[71] A. Kardam, K.R. Raj, S. Srivastava, M.M. Srivastava, Nanocellulose fibers for biosorption of cadmium, nickel, and lead ions from aqueous solution, Clean Technol. Environ. Policy, 16 (2014) 385–393.
[72] N.U. Udeh, J.C. Agunwamba, Equilibrium and kinetics adsorption of cadmium and lead ions from aqueous solution using bamboo based activated carbon, Int. J. Eng. Sci., 6 (2017) 17–26.
[73] I. Abdelfattah, F. El Sayed, A. Almedolab, Removal of heavy metals from wastewater using corn cob, Res. J. Pharm. Biol. Chem. Sci., 7 (2016) 239–248.
[74] R. Karthik, S. Meenakshi, Chemical modification of chitin with polypyrrole for the uptake of Pb(II) and Cd(II) ions, Int. J. Biol. Macromol., 78 (2015) 157–164.
[75] S. Pap, J. Radonić, S. Trifunović, D. Adamović, I. Mihajlović, M.V. Miloradov, M.T. Sekulić, Evaluation of the adsorption potential of eco-friendly activated carbon prepared from cherry kernels for the removal of Pb^{2+}, Cd^{2+} and Ni^{2+} from aqueous wastes, J. Environ. Manage., 184 (2016) 297–306.
[76] D. Imessaoudene, N. Bensacia, F. Chenoufi, Removal of cobalt(II) from aqueous solution by spent green tealeaves, J. Radioanal. Nucl. Chem., 324 (2020) 1245–1253.